Lanthanum oxycarbonate modified Cu/Al_2O_3 catalysts for selective hydrogenolysis of glucose to propylene glycol: base site requirements

P. Yazdani,[a,b] B. Wang,[a] Y. Du,[a] S. Kawi,[b*] A. Borgna[a,b*]

This work reports on the base property of $La_2O_2CO_3$-Cu/Al_2O_3 catalysts and its effect on the catalyst performance for the aqueous hydrogenolysis of glucose to propylene glycol. The catalysts show promising performance in glucose isomerisation, C-C bond cleavage of fructose and hydrogenation of the resulting fragments. The base property of the catalyst influences the selectivity. More specifically, the basicity of the catalyst facilitates the isomerisation of glucose to fructose and C-C bound cleavage of fructose to produce lighter products. This is evidenced by the correlation between acid-base properties of the catalysts and the catalytic performance. In contrast, acid sites promote side reactions such as condensation reactions. Based on this study, a surface reaction mechanism is proposed for the first step of the tandem reactions; the isomerisation of glucose to fructose. The effect of the reaction time and temperature on the product distribution was investigated to get more insight into the reaction pathways. In this regards, the conversion of intermediates was also investigated. Then, a reaction mechanism is proposed based on the findings of this study and previous works.

Introduction

The production of chemical and fuel still heavily relies on fossil resources as feedstock. However, this long lasting landscape is being challenged by environmental concerns, increasing energy and chemical demands due to the fast population growth in the world, and the limited reserves of fossil resources. Therefore, the utilisation of biomass as a renewable carbon source to replace fossil resource has gained much attention. In this context, cellulose, the most abundant component in the lignocellulosic biomass with a yearly production of nearly 40 billion[1], is considered as a promising renewable feedstock. The building blocks of cellulose are glucan chains, which are glucose polymers. Several processes for conversion of glucose have been reported, including dehydration, reduction, gasification, dry reforming, esterification, and hydrogenolysis[1]. It is important to stress that glucose hydrogenolysis has received much more attention compared to the other processes. The high content of oxygen atoms in the glucose molecule makes it a promising feedstock for producing oxygen containing chemicals such as polyols via hydrogenolysis[2]. Glucose hydrogenolysis involves the cleavage of the C-O and C-C chemical bonds in the molecule of glucose. Then, the hydrogenation of the fragments formed during the chemical bond cleavage can further produce various value-added chemicals. In addition, the uncontrolled reactivity of glucose is the main issue lowering down the carbon balance[2]. Hence, it is required to design effective catalysts to control the selectivity to produce high yield of high value chemicals such as propylene glycol and ethylene glycol.

These polyols are widely used as building blocks for production of polymers such as polyethylene terephthalate, polyester resins and other industrial chemicals[3]. It is worth noting that the use of propylene glycol is growing over ethylene glycol due to the toxicity of ethylene glycol to humans and animals[4]. Considering this fact and the higher price of propylene glycol compared to ethylene glycol, significant efforts have been devoted to develop new catalysts for the hydrogenolysis of cellulose/glucose to produce propylene glycol as major product. Several authors reported the reaction mechanism for glucose hydrogenolysis[5-8]. A simplified reaction pathway is depicted in Scheme 1 based on the results of this work and literature. Glucose initially undergoes isomerisation to form fructose, being this step catalysed by Lewis acid or base sites[9]. Subsequently, retro-aldol condensation takes place to convert fructose to C_3 chemicals, including glycerol, pyruvaldehyde, and lactic acid[10-12]. Finally, propylene glycol is produced by hydrogenation of pyruvaldehyde via acetol as an intermediate. Hence, the conversion of glucose to propylene glycol needs a bifunctional catalyst, which could catalyse isomerisation, retro-aldol condensation, dehydration, and hydrogenation reactions. In addition to the mentioned cascade reactions, there are other competing reactions including hydrogenation of glucose and fructose to hexitols, degradation of glucose to ethylene glycol and erythritol, dehydration of fructose to 5-hydroxymetylfurfural, and formation of humins and soluble condensation products[13]. Therefore, precise control of the catalyst properties is required to achieve high yield of propylene glycol.

[a] *Heterogeneous Catalysis Division, Institute of Chemical and Engineering Sciences, A*STAR , 627833, Singapore*
[b] *Department of Chemical and Biomolecular Engineering, National University of Singapore, 119260, Singapore*
*Corresponding authors

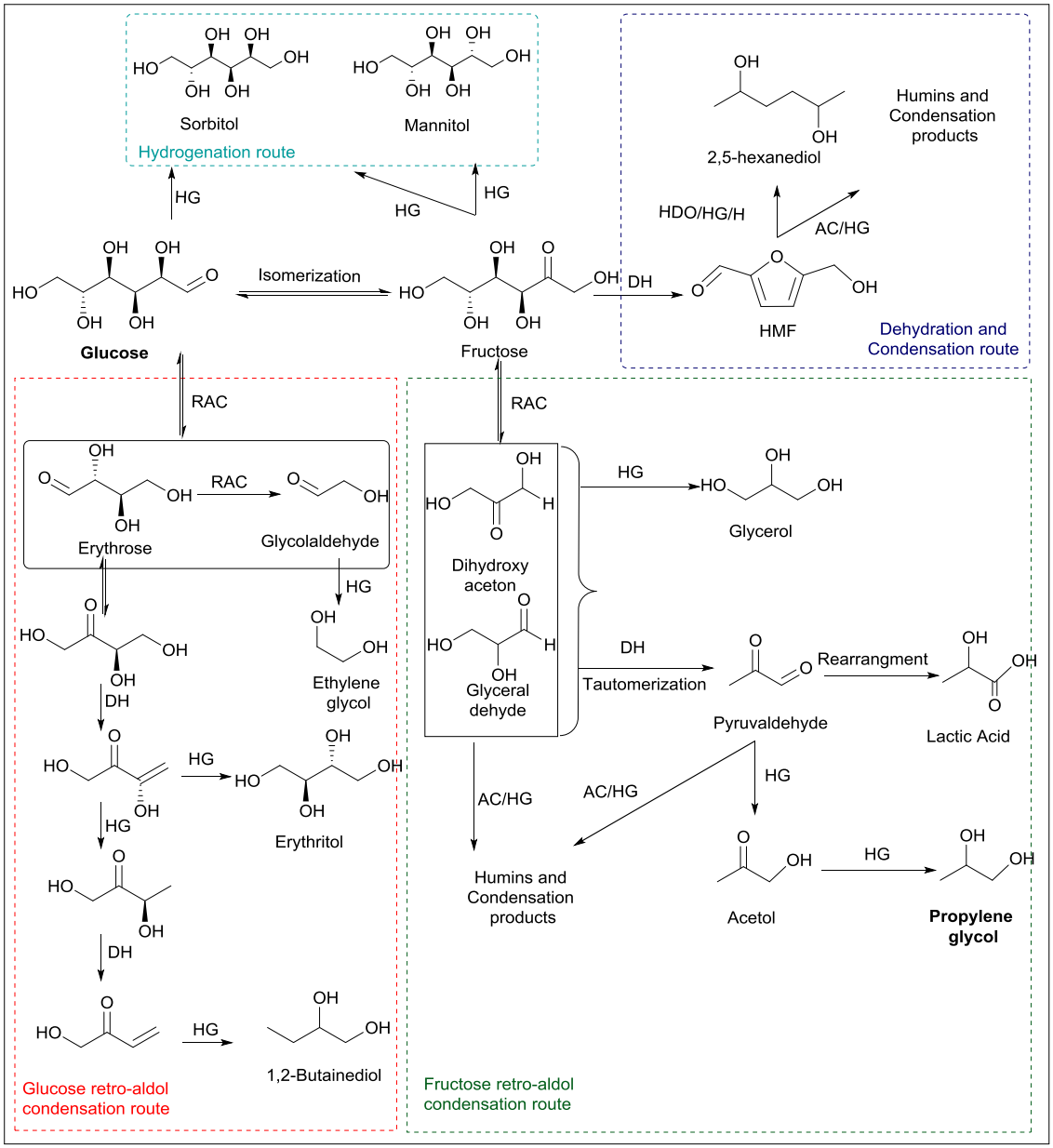

Scheme 1. Proposed reaction pathways for glucose hydrogenolysis towards propylene glycol and by-products adapted from[6, 7, 14]; HG, hydrogenation; H, hydrolysis; DH, dehydration; RAC, retro-aldol condensation; HDO, hydrodeoxygenation; AC, aldol condensation.

Based on these considerations, the development of heterogeneous catalyst with a suitable balance between acid/base properties and selective hydrogenation sites has received considerable attention recently[15]. For instance, several more selective catalysts towards propylene glycol than ethylene glycol have been reported: Ni-SnO_x/Al_2O_3[11], Ni/Ac+SnO[16], Ru/Ac+ZnO[17], $CuO/ZnO/Al_2O_3$[8], and Ni/ZnO[18]. Selectivities towards propylene glycol between 18.4% and 34% were obtained. Those studies have shown that switching the reaction pathway towards the production of propylene glycol can be achieved using appropriate base promoters. Another strategy was to perform the hydrogenolysis of glucose/cellulose over dual system consisting of a homogenous base promoter and a heterogeneous supported metal catalyst. Thus, the hydrogenolysis of cellulose over Cu/CrO_x+$Ca(OH)_2$ gave 42.6% of propylene glycol at 245 °C and 60 bar of H_2[19]. Cellulose hydrogenolysis over Ni/Ac+$La(OH)_3$ produced 27.3% and 25.1% propylene glycol and ethylene glycol at 245 °C and 50 bar, respectively[12]. More recently, dual association of $Pt/BaZrO_3$ with $CeCl_3{\cdot}7H_2O$ resulted in 19.2% and 21.7% propylene glycol and ethylene glycol, respectively, when the hydrogenolysis of cellulose was carried out at 230 °C and 25 bar of H_2[10].

Cu/C and Pd/C were reported to be more selective to propylene glycol compared with other transition metals supported on carbon[20]. It is worth noting that the ultimate aim

of this study is to produce propylene glycol as the main product by glucose hydrogenolysis in a sustainable manner. Hence, copper, a non-precious and cheaper metal, was chosen over palladium. In addition, heterogeneous base promoted catalysts are a better choice than homogeneous catalysts in view of alkali separation or neutralization, and corrosion issues[21]. Based on these concerns and inspired by previous reports, Cu-$La_2O_2CO_3$/Al_2O_3 catalysts were developed for glucose hydrogenolysis, allowing the production of propylene glycol from glucose via a more sustainable route. Lanthanum oxide has been used as a promoter in various catalytic reactions[22-24]. The basicity of lanthanum oxide makes it a suitable additive in hydrogenolysis of glucose to propylene glycol[25, 26]. However, dissolution of lanthanum ions in the reaction medium promotes glucose degradation towards ethylene glycol[12]. To overcome this issue, the metal active phases are usually supported on the carriers such as TiO_2, carbon, and Al_2O_3 to improve the hydrothermal stability. Moreover, it was reported that mixed oxides had better stability compared to the corresponding pure oxides in hot liquid water (>200 °C)[27, 28]. In addition, some other studies showed that the thermal stability of aluminium oxide was increased after modification with rare earth metal oxides such as lanthanum oxide[22, 28]. Hence, in this study, both copper and lanthanum were deposited on alumina support by co-precipitation method, where copper provides the hydrogenation site.

Cu-$La_2O_2CO_3$/Al_2O_3 catalysts with different Cu/La ratios were investigated in this work. This approach allows for the correlation of acid/base properties of the catalysts with product distribution during glucose hydrogenolysis to understand the role of the different active sites. In addition, hydrogenolysis of intermediates such as fructose, pyruvaldehyde, and acetol over the developed catalyst was investigated to gain more insights on the reaction mechanism.

Experimental

Catalyst preparation

Cu-$La_2O_2CO_3$/Al_2O_3 catalysts with different Cu/La ratios along with a Cu/$La_2O_2CO_3$ sample were prepared by the co-precipitation method described by Xin Jin et al.[6]. Nitrate precursors of copper, lanthanum, and aluminium were added to deionised water. The amounts of the copper and aluminium precursors used to synthesize 30%Cu/Al_2O_3 were 1.6 and 11.6 gram in 200 ml of water, respectively. Catalysts with Cu/La molar ratios of 9, 6, 3 and 1.5 were prepared by adding 0.33, 0.5, 1.0, 2.0 gram of the lanthanum precursor. The amount of copper and lanthanum precursors used to synthesize 30%Cu/$La_2O_2CO_3$ were 4.7 and 8.7 gram, respectively. Another solution was prepared by dissolving 3.0 of 25.4 gram of sodium hydroxide and sodium carbonate in 300 ml of deionised water. The prepared solutions were added drop wise to the solution of the nitrate precursors, which was kept at 60 °C in a silicon oil bath under vigorous stirring. The pH of the solution was kept above 10 during the precipitation. The solution was then aged at 60 °C for 16 hours under vigorous stirring. Subsequently, warm deionised water (70 °C) was added to the solution until the pH of the solution decreased to 7. The precipitated solids were obtained by filtration and dried overnight at 100 °C in a vacuum oven. The dried catalysts were then calcined at 400 °C for 5 hours using a heating ramp of 1 °C /min in following air. The activation of the catalysts was performed at 400 °C for 2 hours with a ramping rate of 2 °C /min in hydrogen flow. Finally, the reduced catalyst was passivated using a mixture of 1%O_2 in N_2 for 30 min before exposure to ambient air. The prepared catalysts were designated by the theoretical Cu/La molar ratio.

Catalytic activity

The hydrogenolysis of glucose was carried out in a 300 ml stirred Parr-reactor with teflon liner under 34 bar of H_2 gas. High pressure of H_2 gas was introduced in the parr reactor before heating up the reactor to the reaction temperature. The heating time to 200 °C was 35 min. Time zero was taken as the time at which temperature reached to 200 °C. The resulting solution obtained after reaction was analysed with HPLC. 0.5 mM aqueous solution of sulfuric acid was used as mobile phase in the HPLC analysis, using a flow rate of 0.5 ml/min. The temperature of the aminex HPX-87H column was kept at 60 °C.

Catalyst characterisation

The powder X-ray diffraction (XRD) patterns were recorded on a Bruker AXS D8 diffractometer using CuKα radiation operating at 40 kV and 40 mA. The diffraction patterns were recorded in the 2θ range of 20-80°. The Brunauer Emmett Teller (BET)-surface area was determined by N_2 physical adsorption at liquid N_2 temperature using a Micromeritics ASAP 2420 system. The pore volume of the catalysts was calculated by BJH method. Prior to BET analysis, the catalysts were pretreated at 200 °C for 2 hours under vacuum. Temperature-programmed reduction (TPR) studies were performed on a Thermo Scientific TPDRO 1100 instrument equipped with a thermal conductivity detector (TCD). Prior to TPR studies, 40 mg of the catalyst powder was outgassed for 1 hour under Ar flow at 100 °C using a ramping rate of 5 °C/min. Then TPR measurements were performed under 30 ml/min flow of 10%H_2/90%Ar from room temperature to 600 °C at a ramping rate of 5 °C/min. Temperature programmed desorption (TPD) of CO_2 was used to determine the total basicity and base strength of the prepared catalysts. Prior to analysis, 100 mg of the catalyst was first flashed with N_2 for 5 min at room temperature followed by reduction in 30 ml/min flow of 5% H_2 at 400 °C for 60 min. After cooling down to 50 °C, the catalyst was saturated with CO_2 (30 ml/min) for 30 min. Physically adsorbed CO_2 was removed using flowing N_2 gas for 30 min. Then, CO_2 TPD was carried out heating up from 50 °C to 800 °C under 30ml/min of flowing He and the desorbed CO_2 was quantified using a TCD. The CO_2-TPD profiles were analysed using multiple Gaussian functions to carry out the fittings. The area of the deconvoluted peaks was calculated using OriginPro

2016 software. NH_3-TPD of was performed to analyse the acidity of the catalysts. Pretreatment and reduction procedures were similar to those used for CO_2-TPD. The reduced catalysts were cooled down to 100 °C and saturated with NH_3 (50ml/min) for 60 min. Then, the sample was treated under 50 ml/min flow of He for 60 min. The acidity of the sample was determined by heating the catalyst from 100 °C to 800 °C under 50ml/min flow of He and the desorbed NH_3 was detected with a TCD. Copper surface area and dispersion of the catalysts were determined by the dissociative N_2O chemisorption as reported elsewhere[29]. The catalysts were pretreated and reduced as previously described for CO_2-TPD method. Then, oxidation of the copper surface was performed by introducing 30 ml/min of N_2O at 80 °C. N_2O was assumed to be dissociated, resulting in the oxidation of two copper atoms. Subsequently, the catalyst was purged with 30 ml/min of N_2 to remove the residual N_2O gas. Then, Cu_2O was reduced by using 30 ml/min flow of 5% H_2 in Ar. X-ray absorption spectra (XAS) of Cu-K edge and La-L_{III} edge were recorded at the XAFCA beam line at the Singapore Synchrotron Light Source[30]. The samples were firstly mixed with boron nitride to prepare the samples. The samples were reduced under similar conditions to those used for the catalyst activation described in the catalyst preparation section. TEM images were taken on a JEM-2100F transmission electron microscope and SEM images of the catalysts were recorded on a JEOL FEG SEM (SM 6700F).

Results and discussions

Textural properties

The physical properties of the catalysts were characterised by N_2O chemisorption and N_2 physisorption methods, and the results are presented in Table 1. As shown in the Table, the surface area and dispersion of the copper particles for Cu/Al_2O_3 catalyst are 53.8 m^2/g and 8.3%, respectively, indicating a copper particle size of 12.5 nm. Interestingly, the surface area and dispersion of the copper particles increase with the addition of lanthanum to the Cu/Al_2O_3 catalyst to 99.6 m^2/g and 15.3%, respectively. In the case of $Cu/La_2O_2CO_3$, they are 63.3 m^2/g and 9.8%, respectively. Hence, the metal dispersion in all Cu-$La_2O_2CO_3/Al_2O_3$ catalysts is higher than that in the Cu/Al_2O_3 catalyst. As a result, smaller copper particles are produced on the surface of the Cu-$La_2O_2CO_3/Al_2O_3$ and $Cu/La_2O_2CO_3$ compared to that of the Cu/Al_2O_3. The mentioned trend is consistent with previous studies on the effect of the lanthanum loading on the crystal growth of nickel particles supported on aluminium oxide[22]. The surface areas of the catalysts with different lanthanum loadings are quite similar, while the area of $Cu/La_2O_2CO_3$ catalyst is only 34.8 m^2/g. This value is much lower than the surface areas of the other catalysts. Thus, it is reasonable to expect that alumina enhances the metal dispersion by providing an increased surface area. Moreover, the addition of lanthanum could further enhance the Cu dispersion.

Table 1. Textural properties of the Cu-$La_2O_2CO_3/Al_2O_3$ catalysts with different Cu/La ratios along with $Cu/La_2O_2CO_3$.

Cu/$La_2O_2CO_3$-Al_2O_3	CuO /La_2O_3 (wt%)[a]	S_{BET} (m^2/g)	d_{pore} (nm)[b]	D (%)[c]	Cu SA (m^2/g)[d]	Cu PS (nm)[e]
Cu/Al_2O_3	22.7/-	94.0	18.6	8.3	53.8	12.5
Cu/La=9.0	22.4/8.	90.0	24.3	11.5	75.1	8.9
Cu/La=6.0	17.9/11	97.7	28.7	14.5	93.8	7.2
Cu/La=3.0	17.6/18	99.2	21.4	14.8	96.3	7.0
Cu/La=1.5	15.4/28	106.9	20.2	15.3	99.6	6.7
$Cu/La_2O_2CO_3$	23.6/60	34.8	25.9	9.8	63.3	10.6

[a] XRF analysis
[b] Pore Diameter (d_{pore}) from BJH method
[c] Cu Dispersion (D) calculated from N_2O chemisorption
[d] Cu Surface Area (SA) calculated from N_2O chemisorption
[e] Cu Particle Size (PS) calculated from N_2O chemisorption

XRD Patterns

Figure 1 compares the XRD patterns of the calcined catalysts. The diffraction pattern corresponding to the monoclinic structure of $La_2O_2CO_3$ (JCPDS 00-048-1113) is observed in all XRD patterns of La-containing catalysts. Moreover, the diffraction peaks appearing at 35.5°, 38.6°, and 66.2° can be indexed to CuO phase (JCPDS 04-012-7238). It is clearly shown that the intensity of the CuO diffraction peaks is decreased with the increase of lanthanum loading and eventually vanished for the catalyst with Cu/La ratio= 1.5. This suggested that the addition of the lanthanum enhance the dispersion of the copper particles on the catalyst surface, being consistent with N_2O chemisorption results.

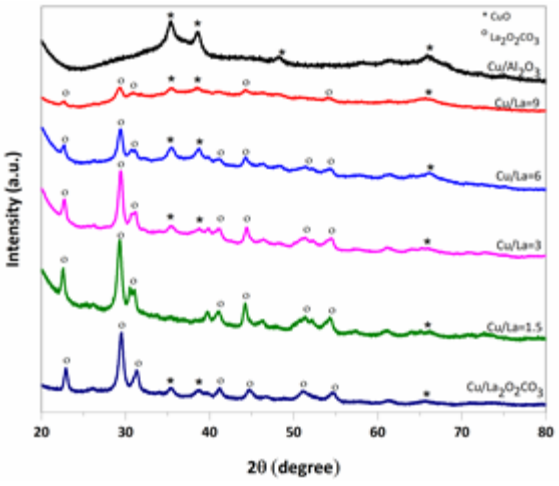

Figure 1. XRD spectra of the calcined catalysts.

.

TEM and SEM images

TEM images of the reduced Cu-$La_2O_2CO_3/Al_2O_3$ with Cu/La ratio at 6 is presented in Figure 2. These images demonstrate that copper particles are spherical in shape, having a wide range of copper particle sizes on the catalyst surface. The average copper particle size is estimated using Nano Measure software over 200 particles. An average particle size of 8.3 nm with a standard deviation of 3.9 nm was obtained. The calculated mean particle size from TEM images is in good agreement with the particle size determined by N_2O chemisorption (Table 1).

SEM images of the calcined catalysts are presented in Figures S1. SEM images reveals that the catalysts prepared in this study are composed of agglomerates with different shapes and sizes in the range of 10-50 µm. SEM-EDX pattern were also measured and presented in the Figure S2. EDX analysis confirmed that both Cu and La atoms are present on the surface of the calcined catalysts. The concentration of the copper particles on the surface of the catalysts decreases from 31.2wt% to 10.6wt% by increasing the lanthanum loading from 0 to a Cu/La ratio= 1.5, while the concentration of lanthanum increases from 0.0 wt% to 29.2 wt%. The concentration of the Cu and La atoms on the surface of the Cu/ $La_2O_2CO_3$ catalyst are 15.2 wt% and 39.5 wt%, respectively. Hence, SEM images clearly show that upon addition of lanthanum, the concentration of the copper atoms on the surface decreases while the lanthanum concentration increases.

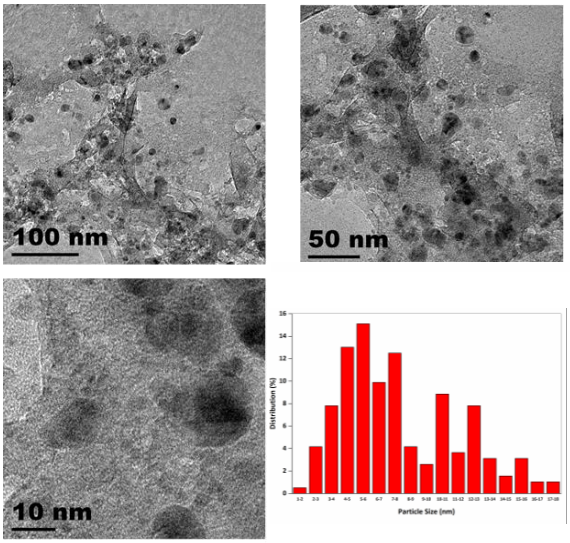

Figure 2. TEM images and particle size distribution of Cu-$La_2O_2CO_3/Al_2O_3$ sample with a Cu/La ratio=6.

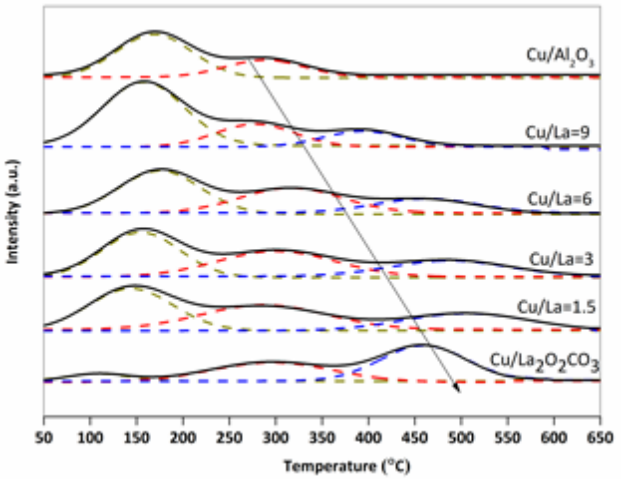

Figure 3. CO_2-TPD profile of the catalysts.

Acid-Base properties

CO_2-TPD profiles of the synthesized catalysts are depicted in Figure 3. It can be seen that there are different desorption peaks in the range of 50-650 °C. These desorption peaks correspond to base sites with different strengths. Table 2 shows the relative concentration of base sites with different strengths, estimated by integrating the area under the deconvoluted peaks. Di Cosimo et al. assigned the desorption peaks of CO_2 at increasing temperature to bicarbonates, unidenate carbonates and bidenate carbonates, adsorbed on hydroxyl groups, metal-oxygen pairs, and oxygen anions, respectively[31]. It is worth noting that all samples possess a similar amount of hydroxyl groups on the surface of the catalysts, except for the Cu/ $La_2O_2CO_3$ catalyst. The concentration of hydroxyl groups on the surface of the Cu/ $La_2O_2CO_3$ catalyst is 0.08 µmol/m^2, while for other catalysts it is between 0.56-0.62 µmol/m^2 (Table 2). Meanwhile, the concentration of the moderate and strong base sites clearly increases as the loading of the lanthanum increases, reaching the highest value for the Cu/ $La_2O_2CO_3$ catalyst. In contrast, the NH_3-TPD profiles of the catalysts only possess one peak at 200 °C. The concentration of these weak acid sites, calculated from the integration of the NH_3-TPD profile, is presented in Table 2. Clearly, the concentration of acid sites decreases as a result of the increasing lanthanum loading. Moreover, Cu/ $La_2O_2CO_3$ catalyst does not possess acid sites. In summary, the acid/base properties of the catalysts can be effectively modified by changing the Cu/La/Al ratio.

Table 2. Concentration of base and acid sites on the catalyst surface

Cu-La-Al Mixed oxides	Concentration of basic sites, µmol/m^2			Concentration of acid sites, µmol/ m^2
	Weak	Moderate	Strong	
Cu/Al_2O_3	0.56	0.22	-	0.45
Cu/La=9.0	0.62	0.33	0.23	0.16
Cu/La=6.0	0.61	0.44	0.25	0.12
Cu/La=3.0	0.60	0.52	0.32	0.05
Cu/La=1.5	0.61	0.53	0.37	0.05
$Cu/La_2O_2CO_3$	0.08	0.4	0.52	-

TPR profiles

TPR profiles of the catalysts are depicted in Figure 4. All catalysts display a broad reduction peak in the temperature range of 200-330 °C. Two reduction peaks are observed at low temperature for Cu/Al_2O_3, which can be assigned to the two step reduction of the bulk CuO, whereas the peak observed at higher temperatures is ascribed to well-dispersed CuO particles strongly interacting with the support[32]. As shown in Figure 4, copper oxide reduces at higher temperature when it is supported on alumina as compared to $La_2O_2CO_3$-supported copper oxide. This can be ascribed to the stronger interaction of the copper oxide species with alumina. Interestingly, promoting the Cu/Al_2O_3 with relatively small amounts of lanthanum oxycarbonate (Cu/La=9, 6 and 3), shifts the reduction of copper oxide to higher temperature due to the increasing CuO dispersion. Thus, stronger interaction between CuO species and alumina clearly exist because of the higher dispersion of CuO species in presence of lanthanum oxycarbonate. However, the reduction temperature of the CuO- $La_2O_2CO_3/Al_2O_3$ sample with Cu/La=1.5 is shifted to lower temperatures as a results of the week interaction between copper and lanthanum oxycarbonate. Therefore, it is clear that the reduction of copper oxide species is strongly affected by addition of the lanthanum and it depends on the lanthanum loading. Indeed, some contradictory observations of the effect of lanthanum oxide on the reducibility of metals were reported in the literature as well. The delay of Ni reduction by lanthanum oxide was reported by Znak et al.[33] and Liu et al.[24], while others reported that lanthanum oxide facilitates the reduction of nickel and copper[22, 34, 35]. Herein, our results indicate that the reducibility of the CuO- $La_2O_2CO_3/Al_2O_3$ catalysts depends on the loading of lanthanum oxycarbonate.

XPS and XAS Characterisations

Copper 2p core level XPS spectra of the calcined catalysts are shown in Figure 5. These samples exhibit the Cu $2p_{3/2}$ and Cu $2p_{1/2}$ peaks at the binding energy of 933.9 eV and 954.2 eV, respectively. A sharp satellite peak is observed in the XPS spectra of the catalysts, indicating the presence of the CuO on the surface of the samples.

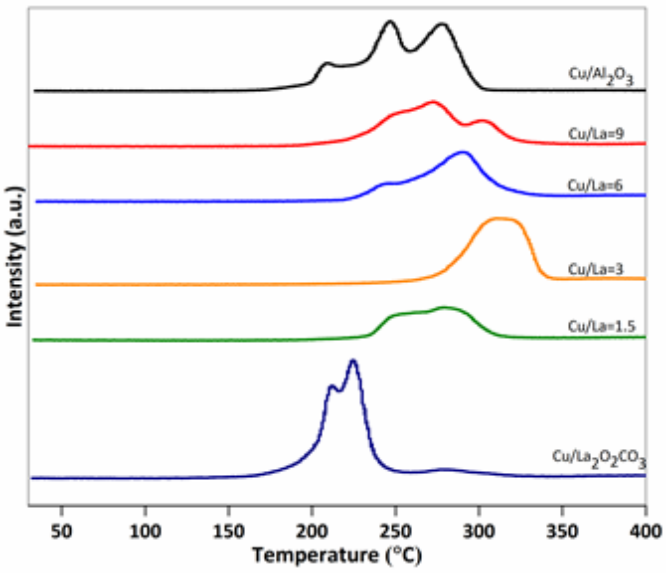

Figure 4. TPR profiles of the catalysts.

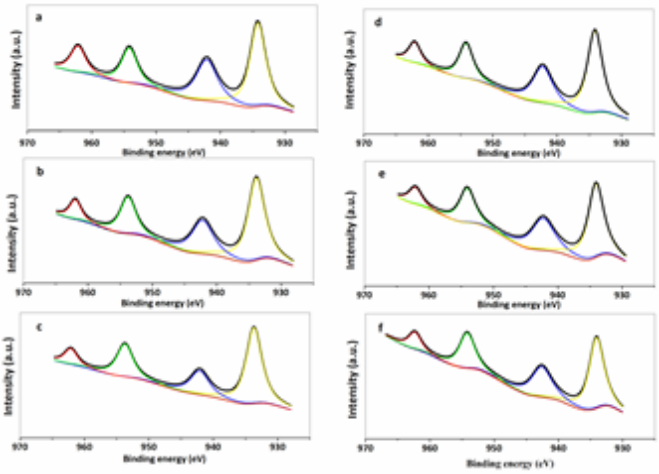

Figure 5. Copper 2p core level XPS spectra of the calcined catalysts, a) Cu/Al_2O_3, b) Cu/La=9, c) Cu/La=6, d) Cu/La=3, e) Cu/La=1.5, f) Cu/ $La_2O_2CO_3$.

It is worth noting that the chemical state of copper oxide is not affected by the presence of lanthanum oxycarbonate, as no change in the binding energy of Copper 2p core level XPS spectrum is observed.

X-ray absorption spectroscopy (XAS) was employed to measure the local structure and electronic states of copper and lanthanum species in the synthesized catalysts. The Fourier Transforms (FT) of Cu K-edge EXAFS spectra of the calcined catalysts along with CuO as reference are compared in Figure 6a. These results confirm that copper species on the surface of the calcined catalysts exist only as CuO, which is consistent with XRD diffraction patterns and XPS data. Hence, the electronic state of the copper species is not significantly influenced by lanthanum oxycarbonate and alumina support after the calcination. The FTs of the EXAFS spectra for the reduced catalysts are compared with metallic copper in Figure 6b. This Figure shows that CuO is reduced to the metallic copper in all samples after reduction at 400 °C for 2 hour, being Cu° the active site for hydrogenation. The curve fitting of Cu K-edge EXAFS of the catalysts reduced at 400 °C shows the existence of Cu-Cu distances at 2.50-2.51 Å and coordination numbers (CN) of ca. 10 ± 1 (Table S1). The fitting parameters of the catalysts are summarised in Table S1. These results indicate that there is no evidence of copper-lanthanum interaction. In addition, it is worth noting that the coordination numbers obtained by the fitting procedures indicate the presence of relatively large Cu particles with particle sizes > 4 nm[36]. Figure 7 shows the La L_{III} XANES spectra of $La_2O_2CO_3$ and the reduced catalysts. The XANES spectra of the catalysts are similar to that of the bulk lanthanum oxide. However, the white line intensity for the synthesized catalysts is slightly higher when it is compared with bulk lanthanum oxide. This feature suggests the modification of the electronic structure of the lanthanum cations, resulting from the interaction between lanthanum oxycarbonate and the support[37].

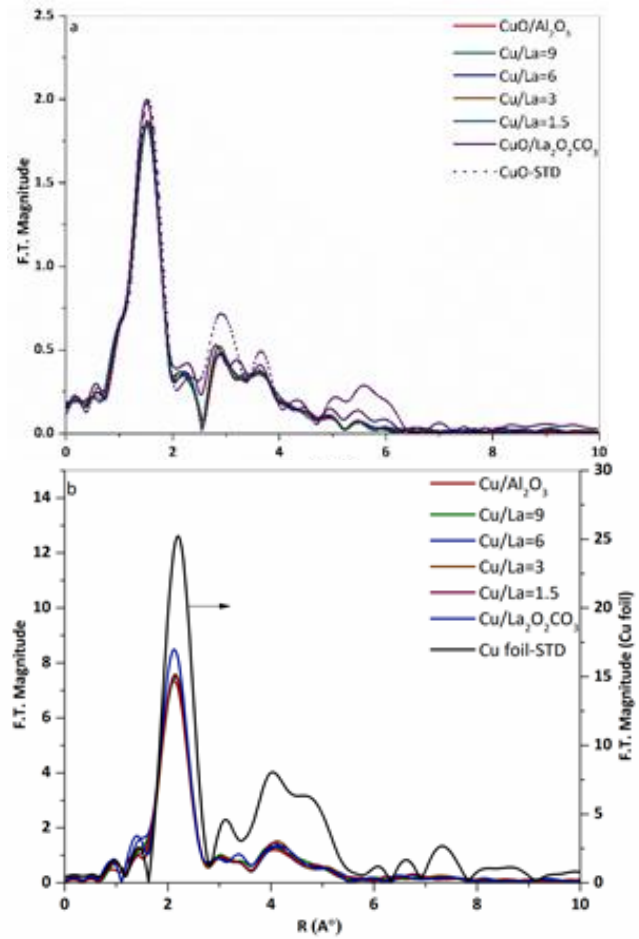

Figure 6. Cu K-edge EXAFS spectra of a) CuO/ $La_2O_2CO_3$-Al_2O_3 with different ratio of Cu/La, and CuO/ $La_2O_2CO_3$, b) Cu/ $La_2O_2CO_3$-Al_2O_3 with different ratio of Cu/La, and Cu/ $La_2O_2CO_3$.

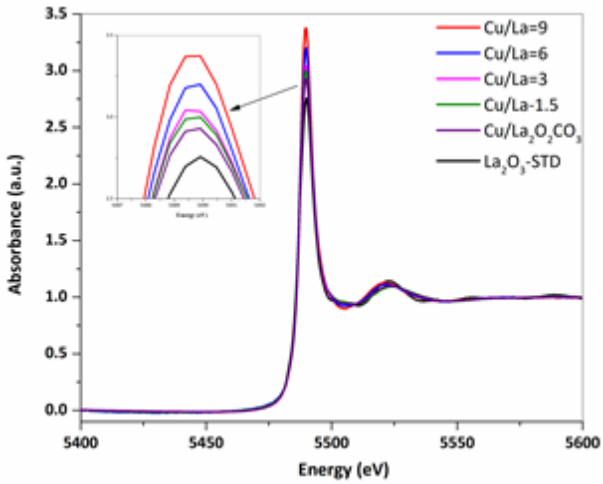

Figure 7. XANES spectra of the reduced Cu-$La_2O_2CO_3$/Al_2O_3 with different Cu/La ratios and Cu/ $La_2O_2CO_3$ at the La L_{III}-edge.

Catalytic Results

The performance in glucose hydrogenolysis of the Cu-$La_2O_2CO_3$/Al_2O_3 catalysts with different Cu/La ratios along with the Cu/ $La_2O_2CO_3$ catalyst is compared in Table 3. 5-hydroxyl methyl furfural is the main product in the blank experiment, yielding 25.2% after 10 min reaction at 200 °C and 34 bar of H_2 (Table 3, entry 10). The conversion of glucose to 5-hydroxylmethylfurfural was reported by several authors[2, 18] under similar reaction conditions applied in this study. As it was reported, glucose easily undergoes transformation under our reaction conditions. Thus, the formation of 5-hydroxymethylfurfural and soluble condensation products is dominant in absence of catalyst[18]. On the contrary, 5-hydroxymethylfurfural selectivity is dramatically decreased in the presence of a catalyst, being glucose fully converted within 10 minutes at 200 °C and 34 bar of H_2 (Table 3, entry 1-6).

Over Cu/Al_2O_3, the main product is sorbitol (34.1% yield) and the total selectivity towards C_3 chemicals, including glycerol, lactic acid, acetol, and propylene glycol, is only 24.2%. This result shows that the concentration of base sites over Cu/Al_2O_3 was not enough to produce propylene glycol as the main product over sorbitol. Zheng et al.[15] also reported that alumina is not effective to promote retro-aldol condensation of glucose, in line with our catalytic results. In addition, minor products such as ethylene glycol (2.4%), fructose (2.3%), arabitol (5.0%), erythritol (1.8%), 1,2-butanediol (2.1%), and 2,5-hexanediol (0.5%) are also detected. The mass balance of the reaction products analysed by HPLC is 73.0% in this case. Low carbon balances have also been reported in several studies on glucose hydrogenolysis to propylene glycol in batch reactors[11, 12, 18, 19]. The carbon loss is ascribed to unidentified and/or undetected products by HPLC analysis, most likely soluble condensation products and humins. These chemicals are produced via the reaction between glucose with HMF and/or HMF with 2,5-dioxo-6-hydroxy-hexanal (hydrated HMF)[13]. In addition, the formation of gas products is not the main reason to explain the low carbon balance, as the difference between total organic carbon (TOC) of the reaction products and feedstock is lower than 5%, as determined by TOC analysis.

Notably, upon addition of lanthanum oxycarbonate, the total selectivity towards C_3 chemicals increases with the concurrent decreasing of the sorbitol yield. This trend indicates that lanthanum oxycarbonate facilitates glucose conversion to propylene glycol. However, selectivity towards lactic acid increases to 15.3% by increasing the Cu/La ratio from 9.0 to 1.5. Moreover, over the catalyst without alumina ($Cu/La_2O_2CO_3$), the total yield of (acetol + propylene glycol) is 40.1 %. Clearly, aluminium oxide plays the role of support for copper and lanthanum oxycarbonate, as evidenced by comparing the catalytic results of Cu/Al_2O_3 and $Cu/La_2O_2CO_3$. Hence, a proper balance of base sites and hydrogenation sites is required to facilitate glucose hydrogenolysis to acetol and minimise the yields of by-products such as sorbitol and lactic acid. In addition a proper ratio of acid sites and base sites (Cu/La=6) is required to maximised the carbon balance, as evidenced by carbon balance results presented in Table 3 along with the characterisation results Therefore, the reaction time of glucose hydrogenolysis over these two catalysts (Cu/La ratio of 6 and $Cu/La_2O_2CO_3$) was extended to 3 h to convert acetol into propylene glycol and the catalytic results are shown in entry 7-8, Table 3. Propylene glycol yields over these catalysts reach 29% and 32%, being comparable to the highest yields reported in the literature[5, 17-19]. It is worth noting that propylene glycol yield exceeds the yield of ethylene glycol over these catalysts at 200 °C and 34 bar of H_2. These reaction results are in contrast with those obtained during cellulose hydrogenolysis over Ni/C+LaOH at 245 °C and 50 bar of H_2, where ethylene glycol was reported as the main product by Sun et al[12]. They have shown that lanthanum ions in solution, acting as a homogenous catalyst, along with a Ni/C heterogeneous catalyst directed the reaction pathway towards ethylene glycol production. So, an experiment was designed to determine if, in our case, the reaction proceeds over lanthanum ions dissolved in the reaction media. In order to verify this, Cu- $La_2O_2CO_3/Al_2O_3$ with a Cu/La ratio= 6 was treated in water at 200 °C and 34 bar of H_2 for 10 min. Then, the reaction media was separated from the solid catalyst using a centrifuge. Then, glucose was added to the solution and used in a blank experiment (entry 11, Table 3). In this experiment, acetol yield is 6.1% and the carbon balance is only 46.4%, which is much lower than the one obtained in the blank experiment reported in entry 10 of Table 3. Hence, this result clearly suggests that glucose hydrogenolysis to acetol in this study is catalysed by a heterogeneous catalyst, Cu-$La_2O_2CO_3/Al_2O_3$, other than the homogeneous lanthanum ions. In addition, retro-aldol condensation of fructose is favoured under our reaction conditions, resulting in the production of propylene glycol as the main product.

Glucose hydrogenolysis over commercial La_2O_3 was also examined to understand the role of $La_2O_2CO_3$ and Cu individually. These catalytic results are presented in entry 9, Table 3. It shows that the main product of glucose hydrogenolysis over La_2O_3 is lactic acid with yield of 42.0%. Acetol was produced as well with a yield of 11.5%. This result suggests that lanthanum oxycarbonate is responsible for the glucose isomerisation to fructose and retro-aldol condensation of fructose to C_3 chemicals (Scheme 1). Hence, it can be postulated that lanthanum oxycarbonate, formed on the surface of the synthesized catalyst, plays a similar role during glucose hydrogenolysis. As shown by CO_2-TPD, NH_3-TPD, and XRD, lanthanum oxycarbonate was formed on the surface of the catalyst, changing the catalyst acid/base properties dramatically. This change explains the enhancement of the selectivity towards propylene glycol by controlling the rate of the competitive reactions. Cu/Al_2O_3 contains the lowest basicity and highest concentration of acid sites, being this catalyst less active towards C-C bond cleavage and more active for hydrogenation. Then, higher concentration of moderate and strong base sites, along with lower concentration of acid sites lead to an increase in the selectivity towards acetol and propylene glycol. Hence, base sites play a vital role in producing C_3 chemicals from glucose hydrogenolysis. However, it is difficult to distinguish whether the required active sites are moderate or strong base sites due to the co-existence of both base sites. Therefore, it can only be concluded that the presence of a suitable amount of moderate and strong base sites are required for efficiently promote this reaction. $Cu/La_2O_2CO_3$ contains negligible amounts of weak base sites while the concentration of weak base sites in Cu-La-Al catalysts is similar to the one on Cu/Al_2O_3 catalysts, thus suggesting that weak base sites are not effective to promote propylene glycol production.

Table 3. Catalytic results of glucose conversion over Cu-$La_2O_2CO_3$/Al_2O_3 catalysts.

			Selectivity (%)								
				C_3 chemicals							
Entry	Catalysts	Conversion	Sorbitol	Glycerol	Lactic acid	Acetol	Propylene glycol	Ethylene glycol	HMF	Others[b]	Carbon balance
1	Cu/Al_2O_3	95.5	34.1	13.4	2.4	5.7	2.7	2.4	0.6	11.7	69.8
2	Cu/La=9.0	98.8	9.6	9.8	4.9	18.8	3.5	3.9	-	10.8	60.6
3	Cu/La=6.0	100	3.9	9.6	8.1	36.9	3.1	6.9	-	13.6	82.1
4	Cu/La=3.0	100	2.0	7.3	13.2	37.8	1.1	5.0	-	12.7	79.1
5	Cu/La=1.5	100	2.3	5.5	15.3	39.3	1.0	5.1	-	13.0	81.5
6	Cu/$La_2O_2CO_3$ ~~La_2O_3~~	100	0.8	2.2	14.8	37.9	2.2	3.3	-	8.5	69.7
7	Cu/La=6.0[a]	100	3.3	8.1	8.1	-	29.0	6.9	-	15.2	70.6
8	Cu/$La_2O_2CO_3La_2O_3$[a]	100	1.3	4.1	8.0	-	32.0	7.1	-	16.1	68.6
9	La_2O_3	99.8	-	-	42.1	11.5	1.4	-	-	14.4	69.3
10	Blank 1[c]	63.1	-	-	5.7	0.8	-	-	40.0	18.8	41.6
11	Blank 2[d]	95.5	-	-	6.6	6.4	-	-	15.0	18.4	44.4

Reaction condition: 0.3 wt% glucose in 100 ml water, 0.1 g catalyst, 200 °C, 34 bar of H_2, reaction time: 10 min. [a]Reaction time: 3 hours. [b]Others: ethanol, 1,2-butandiol, erythritol, methanol, 2,5-hexandiol, 2.5-hexanedion, levulinic acid, arabitol, fructose, xylitol. [c]Blank 1, without catalyst. [d]Blank 2, without catalyst and using water previously contacted with a Cu-$La_2O_2CO_3$/Al_2O_3 catalyst for 10 min at 200 °C and 34 bar of H_2 as described above.

The mentioned correlation between catalytic results and acid/base properties of the catalysts are further considered to understand the mechanism of the glucose isomerisation to fructose. It is known that this reaction follows two different mechanisms: proton transfer and hydride shift[38, 39]. Proton transfer involves base catalysed deprotonation of the carbonyl group in the glucose molecule, known as Lobry-de Bruyn-van Ekenstein (LdB–AvE) mechanism. The hydride shift involves the polarization of the carbonyl group of glucose and it is catalysed by Lewis acid sites[9], known as Meerwein-Ponndorf-Verley mechanism. The role of each pathway in the isomerisation of glucose to fructose has been widely debated. The correlation between the catalytic results and the acid-base properties (Figure 8) suggests that glucose isomerisation follows the proton-transfer mechanism, because Cu/$La_2O_2CO_3$ without any acid site converts glucose to propylene glycol, resulting in a yield of 32%. Hence, glucose isomerisation to fructose is believed to follow the LdB–AvE mechanism[38]. Based on this mechanism, base sites of the catalysts deprotonate α-carbonyl carbon of the acyclic glucose to form enolate intermediates. The open-ring form of fructose is then produced by transferring a proton from C_2 to C_1 and O_2 to O_1 of the enolate intermediates, as shown in Figure 9. Then the open chain form of fructose is converted to C_3 chemicals via retro-aldol condensation[40].

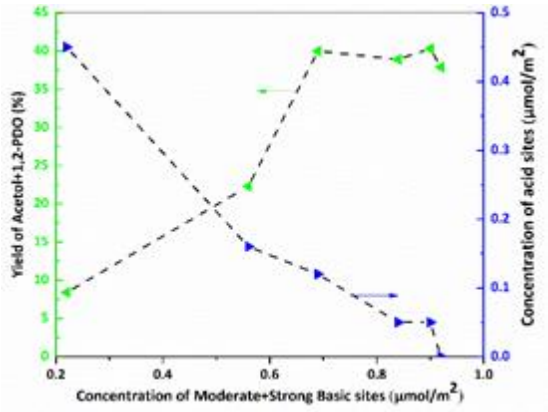

Figure 8. Correlation between acid/base properties of the catalysts and the yield of acetol + propylene glycol.

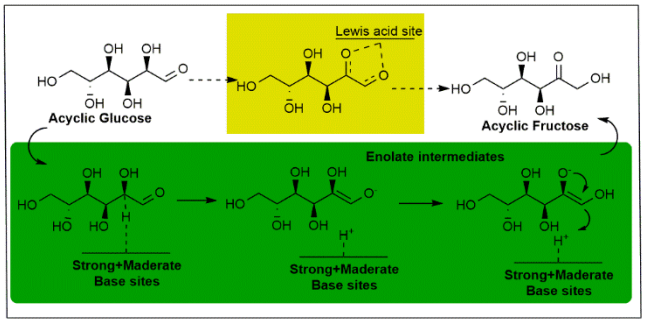

Figure 9. Proposed reaction mechanism adapted from previous reports[9, 38, 39] for glucose isomerisation to fructose over the synthesized catalysts.

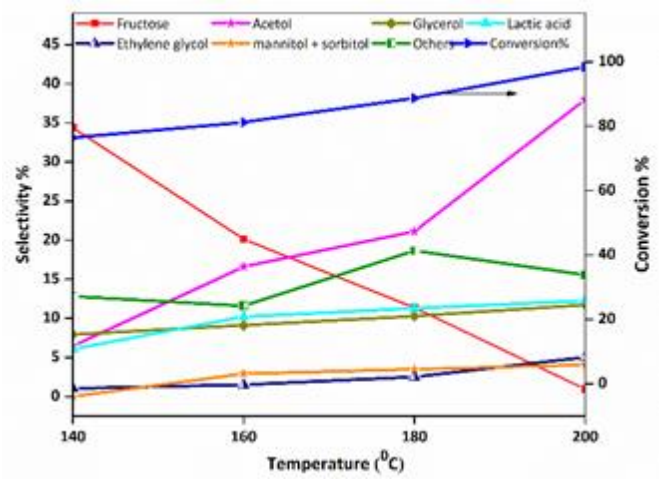

Figure 10. Product distribution of glucose hydrogenolysis over Cu-$La_2O_2CO_3/Al_2O_3/Al_2O_3$ with a Cu/La ratio=6 during heating up of the reactor, reaction condition: 0.3wt% glucose, 0.1 g catalyst, 100 ml water, 34 bar of H_2, others: arabitol, xylitol, erythritol, pyruvaldehyde, methanol, HMF, 2,5-hexanediol, levulinic acid.

Effect of temperature and reaction time

The effect of reaction time and temperature on the product distribution over Cu-$La_2O_2CO_3/Al_2O_3$ with a Cu/La ratio= 6 was investigated to get more insight into the reaction pathway. The product distribution of glucose hydrogenolysis during the heating process is shown in Figure 10 and the product distribution of increasing reaction times at 200 °C is depicted in Figure 11.Figure 10 shows that 76.4% of glucose is converted to various products during the heating process from room temperature to 140 °C. At this conversion, fructose is the main product with a selectivity of 34.3% while the selectivity towards C_3 chemicals is 21.6%. However, fructose is completely converted completely to C_3 chemicals and other products by further increasing the temperature to 200 °C, evidenced by an increase of selectivity towards C_3 chemicals to 66.2%, indicating that the retro-aldol condensation of fructose to C_3 chemicals is effectively promoted. Thus, the rate-limiting reaction step of these tandem reactions towards propylene glycol would be the acetol hydrogenation step. As shown in Figure 11, the hydrogenation of acetol proceeds when the reaction temperature reaches 200 °C. After 3 h, the hydrogenation of the acetol at 200 °C resulted in a 30% yield of the propylene glycol, remaining fairly constant afterwards. Degradation products of propylene glycol such as 1-propoanol and 2-propanol are not detected even after 6 hour reaction. This suggests that propylene glycol is stable under our reaction conditions. Glycerol and lactic acid are produced with yields of 11.7% and 12.2%, respectively, during the heating process, remaining almost constant afterwards. Sugar alcohols such as sorbitol, mannitol, arabitol, xylitol, erythritol are also produced during heating process with a total selectivity of 15%.

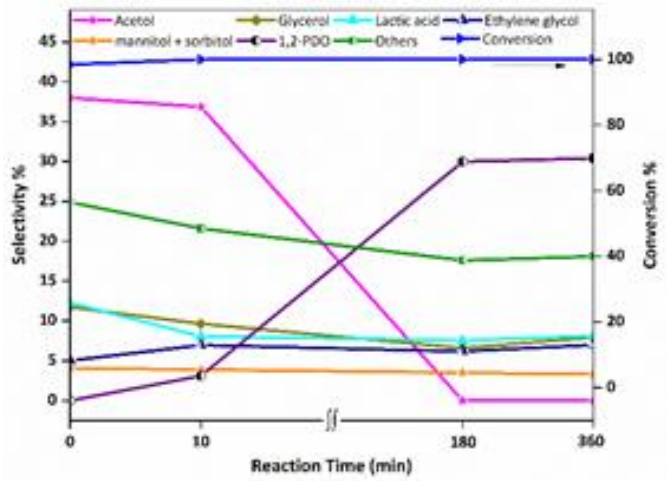

Figure 11. Product distribution-time profile of glucose hydrogenolysis over Cu- $La_2O_2CO_3/Al_2O_3/Al_2O_3$ with a Cu/La ratio=6, reaction condition: 0.3wt% glucose, 0.1 g catalyst, 100 ml water, 34 bar of H_2, others: arabitol, xylitol, erythritol, pyruvaldehyde, methanol, HMF, 2,5-hexanediol, levulinic acid.

Table 4. Hydrogenolysis of the reaction intermediates over Cu-$La_2O_2CO_3/Al_2O_3/Al_2O_3$ with a Cu/La ratio= 6

Entry	Feed	Conversion%	Selectivity%					
			Glycerol	Lactic acid	Acetol	Propylene glycol	Ethylene glycol	Others
1	Fructose	100	6.8	6.2	36.7	-	5.1	12.2
2	Acetol[a]	72.9	0	10.5	-	76.6	0	2.0
3	Pyruvaldehyde	100	-	26.1	29.2	-	-	-

Reaction condition: 0.3 wt% feed solution, 100ml water, 0.1 g Cu- $La_2O_2CO_3/Al_2O_3Al_2O_3$ with Cu/La=6, 200 °C, 34 bar of H_2 and reaction time: 10 min. Others: Ethanol, 1,2-Butandiol, Erythritol, Methanol, 2,5-hexandiol, 2.5-hexanedion HMF, Levulinic acid, Arabitol, Fructose, Xylitol. a) Reaction time: 2 hours.

These chemicals are not further converted by increasing the reaction time to 6 h. One of the competitive reactions for the isomerisation of glucose to fructose under our reaction conditions is the retro-aldol condensation of glucose to ethylene glycol and erythritol. The yield towards erythritol and ethylene glycol reaches to 1.0% and 6.9%, respectively, implying that retro-aldol condensation of glucose is minimal.

In summary, fructose, pyruvaldehyde, and acetol were identified as reaction intermediates. In order to obtain more insights in the reaction mechanism, hydrogenolysis of these intermediates over the Cu- $La_2O_2CO_3/Al_2O_3/Al_2O_3$ catalyst with a Cu/La ratio= 6 under the same reaction conditions were carried out and are presented in Table 4. This table shows that product distribution of fructose hydrogenolysis is similar to that of the glucose. Acetol is produced with yield of 36.7% after 10 min at 200 °C. Moreover, acetol is selectively converted to propylene glycol (Table 4, entry 2), resulting in 72.9% of acetol converted with selectivity of 76.6% after 2 hours reaction. On the other hand, pyruvaldehyde is fully converted after 10 min. Acetol and lactic acid with 29.2% and 26.1% yield, respectively, are produced as a result of pyruvaldehyde hydrogenolysis (Table 4, entry 3). It is important to note that a poor mass balance was obtained for this reaction and unidentified peaks in the HPLC were observed within the retention times of glucose hydrogenolysis products. The poor mass balance of pyruvaldehyde hydrogenolysis shows that pyruvaldehyde is also involved in condensation reactions[13].

Conclusion

In this study, the development of a bifunctional catalyst for hydrogenolysis of glucose to propylene glycol is reported. The effect of the relative concentration of base sites and hydrogenation sites on the surface of the catalyst is discussed. Catalytic results and catalyst characterisations validate that the selectivity towards acetol, the precursor of propylene glycol, in the hydrogenolysis of glucose is promoted by moderate and strong base sites on the catalyst. In contrast, the acid sites on the catalysts surface catalyse the reaction towards condensation products, consequently decreasing the overall yield of the desired product. Moreover, the reaction mechanism is proposed based on the parametric studies. It is worth noting that propylene glycol is produced as the main product over sorbitol and ethylene glycol.

Conflicts of interest

There are no conflicts to declare.

Acknowledgements

The authors gratefully thank The Agency for Science, Technology and Research (A*STAR) of Singapore, The National University of Singapore, and NEA (ETRP 1501 103) for their generous financial supports. P.Yazdani is also grateful to A*STAR for the Singapore International Graduate Award (SINGA) scholarship.

References

1. S. Van de Vyver, J. Geboers, P. A. Jacobs and B. F. Sels, *ChemCatChem*, 2011, **3**, 82-94.
2. M. Schlaf and Z. Zhang, *Reaction pathways and mechanisms in thermocatalytic biomass conversion I: Cellulose structure, depolymerization and conversion by heterogeneous catalysts*, Springer 2015.
3. A. Marinas, P. Bruijnincx, J. Ftouni, F. J. Urbano and C. Pinel, *Catalysis today*, 2015, **239**, 31-37.
4. C. Rode, A. Ghalwadkar, R. Mane, A. Hengne, S. Jadkar and N. Biradar, *Organic Process Research & Development*, 2010, **14**, 1385-1392.
5. E. Girard, D. Delcroix and A. Cabiac, *Catalysis Science & Technology*, 2016, **6**, 5534-5542.
6. X. Jin, J. Shen, W. Yan, M. Zhao, P. S. Thapa, B. Subramaniam and R. V. Chaudhari, *ACS Catalysis*, 2015, **5**, 6545-6558.
7. B. O. de Beeck, M. Dusselier, J. Geboers, J. Holsbeek, E. Morré, S. Oswald, L. Giebeler and B. F. Sels, *Energy & Environmental Science*, 2015, **8**, 230-240.
8. K. Tajvidi, P. J. Hausoul and R. Palkovits, *ChemSusChem*, 2014, **7**, 1311-1317.
9. R. Nagorski and J. P. Richard, *Journal of the American Chemical Society*, 2001, **123**, 794-802.
10. E. Girard, D. Delcroix and A. Cabiac, *Catalysis Science & Technology*, 2016.

11. T. Deng and H. Liu, *Journal of Molecular Catalysis A: Chemical*, 2014, **388**, 66-73.
12. R. Sun, T. Wang, M. Zheng, W. Deng, J. Pang, A. Wang, X. Wang and T. Zhang, *ACS Catalysis*, 2015, **5**, 874-883.
13. H. Rasmussen, H. R. Sørensen and A. S. Meyer, *Carbohydrate research*, 2014, **385**, 45-57.
14. M. Orazov and M. E. Davis, *Proceedings of the National Academy of Sciences*, 2015, **112**, 11777-11782.
15. M. Zheng, J. Pang, R. Sun, A. Wang and T. Zhang, *ACS Catalysis*, 2017, **7**, 1939-1954.
16. R. Sun, M. Zheng, J. Pang, X. Liu, J. Wang, X. Pan, A. Wang, X. Wang and T. Zhang, *ACS Catalysis*, 2015, **6**, 191-201.
17. Y. Hirano, K. Sagata and Y. Kita, *Applied Catalysis A: General*, 2015, **502**, 1-7.
18. X. Wang, L. Meng, F. Wu, Y. Jiang, L. Wang and X. Mu, *Green Chemistry*, 2012, **14**, 758-765.
19. Z. Xiao, S. Jin, M. Pang and C. Liang, *Green Chemistry*, 2013, **15**, 891-895.
20. C. Liu, C. Zhang, K. Liu, Y. Wang, G. Fan, S. Sun, J. Xu, Y. Zhu and Y. Li, *Biomass and Bioenergy*, 2015, **72**, 189-199.
21. M. Xian, *Sustainable Production of Bulk Chemicals: Integration of Bio-,Chemo- Resources and Processes*, Springer Dordrecht, Netherlands, 2015.
22. H. L. Rotgerink, R. Paalman, J. Van Ommen and J. Ross, *Applied Catalysis*, 1988, **45**, 257-280.
23. R. Kam, C. Selomulya, R. Amal and J. Scott, *Journal of Catalysis*, 2010, **273**, 73-81.
24. H. Liu, H. Wang, J. Shen, Y. Sun and Z. Liu, *Catalysis Today*, 2008, **131**, 444-449.
25. J. Zhang and D. He, *Journal of colloid and interface science*, 2014, **419**, 31-38.
26. S. Sato, R. Takahashi, M. Kobune and H. Gotoh, *Applied Catalysis A: General*, 2009, **356**, 57-63.
27. H. Xiong, H. N. Pham and A. K. Datye, *Green Chemistry*, 2014, **16**, 4627-4643.
28. F. Héroguel, B. Rozmysłowicz and J. S. Luterbacher, *CHIMIA International Journal for Chemistry*, 2015, **69**, 582-591.
29. J. Evans, M. Wainwright, A. Bridgewater and D. Young, *Applied Catalysis*, 1983, **7**, 75-83.
30. Y. Du, Y. Zhu, S. Xi, P. Yang, H. O. Moser, M. B. Breese and A. Borgna, *Journal of synchrotron radiation*, 2015, **22**, 839-843.
31. J. Di Cosimo, Apesteguı, C.´a, M. Ginés and E. Iglesia, *Journal of Catalysis*, 2000, **190**, 261-275.
32. V. D. Dasireddy and B. Likozar, *Fuel*, 2017, **196**, 325-335.
33. L. Znak, K. Stołecki and J. Zieliński, *Catalysis today*, 2005, **101**, 65-71.
34. S. Natesakhawat, O. Oktar and U. S. Ozkan, *Journal of Molecular Catalysis A: Chemical*, 2005, **241**, 133-146.
35. R. Shi, F. Wang, Y. Li, X. Huang and W. Shen, *Green Chemistry*, 2010, **12**, 108-113.
36. A. Borgna, F. Le Normand, T. Garetto, C. Apesteguia and B. Moraweck, *Catalysis letters*, 1992, **13**, 175-188.
37. M. Capitan, M. Centeno, P. Malet, I. Carrizosa, J. Odriozola, A. Marquez and J. Fernandez Sanz, *The Journal of Physical Chemistry*, 1995, **99**, 4655-4660.
38. C. Liu, J. M. Carraher, J. L. Swedberg, C. R. Herndon, C. N. Fleitman and J.-P. Tessonnier, *ACS Catalysis*, 2014, **4**, 4295-4298.
39. Y. Román-Leshkov, M. Moliner, J. A. Labinger and M. E. Davis, *Angewandte Chemie International Edition*, 2010, **49**, 8954-8957.
40. K. Wang, M. C. Hawley and T. D. Furney, *Industrial & engineering chemistry research*, 1995, **34**, 3766-3770.